Available online at www.sciencedirect.com

ScienceDirect

Cement and Concrete Research 36 (2006) 1490 – 1500

Cement and Concrete Research

Lithological influence of aggregate in the alkali-carbonate reaction

A.M. López-Buendía [a,*], V. Climent [b], P. Verdú [a]

[a] AIDICO-Unida Técnica del Mármol, Cami de Castella, 4. 03660-Novelda, Alicante, Spain
[b] AIDICO, Benjamin Franklin, 17. 46980-Paterna, Valencia, Spain

Received 31 August 2005; accepted 29 May 2006

Abstract

The reactivity of carbonate rock with the alkali content of cement, commonly called alkali-carbonate reaction (ACR), has been investigated. Alkali-silica reaction (ASR) can also contribute in the alkali-aggregate reaction (AAR) in carbonate rock, mainly due to micro- and crypto-crystalline quartz or clay content in carbonate aggregate. Both ACR and ASR can occur in the same system, as has been also evidenced on this paper.

Carbonate aggregate samples were selected using lithological reactivity criteria, taking into account the presence of dedolomitization, partial dolomitization, micro- and crypto-crystalline quartz. Selected rocks include calcitic dolostone with chert (CDX), calcitic dolostone with dedolomitization (CDD), limestone with chert (LX), marly calcitic dolostone with partial dolomitization (CD), high-porosity ferric dolostone with clays (FD). To evaluate the reactivity, aggregates were studied using expansion tests following RILEM AAR-2, AAR-5, a modification using LiOH AAR-5Li was also tested. A complementary study was done using petrographic monitoring with polarised light microscopy on aggregates immersed in NaOH and LiOH solutions after different ages. SEM-EDAX has been used to identify the presence of brucite as a product of dedolomitization. An ACR reaction showed shrinkage of the mortar bars in alkaline solutions explained by induced dedolomitization, while an ASR process typically displayed expansion. Neither shrinkage nor expansion was observed when mortar bars were immersed in solutions of lithium hydroxide.

Carbonate aggregate classification with AAR pathology risk has been elaborated based on mechanical behaviours by expansion and shrinkage. It is proposed to be used as a petrographic method for AAR diagnosis to complement the RILEM AAR1 specifically for carbonate aggregate. Aggregate materials can be classified as I (non-reactive), II (potentially reactive), and III (probably reactive), considering induced dedolomitization ACR (dedolomitization degree) and ASR.

Keywords: Carbonate aggregate; Alkali-carbonate reaction; Alkali-silica reaction; Dedolomitization; Concrete

1. Introduction

Alkali-aggregate reaction (AAR) can take place in concrete causing damage, as a result of generation of amorphous phases through the reaction of alkalis existing in cement and the reactive components of aggregate, producing expansion and weakness, and potentially leading to a collapse. Alkali-silica reaction (ASR) is better known and more evident than the alkali-carbonate aggregate reaction (ACR) with no silica. Nevertheless, ACR could be also expected to lead to damage to structures.

Alkali-carbonate aggregate reaction has been related to general AAR with two types of reaction: (1) the reaction of carbonate minerals in an alkaline environment, developing dedolomitization; and (2) the reaction silica associated minerals in carbonate rocks, in fact, alkali-silica reaction (ASR). This paper studies alkali-carbonate aggregate reactions involving carbonate minerals and silica minerals, with some remarks of iron oxy-hydroxides forming carbonate aggregates.

This damage and the implications of dedolomitization has been studied before [1–3]. Damage is affected by the alkalinity, grain size, rock heterogeneity, concrete permeability, as well as the climatic conditions of humidity and temperature [4].

The mechanism of the alkali-carbonate reaction is not known in detail, and there is controversy about its mechanical effects. For example, in a bibliographic review, Katayama [5] concludes that pure ACR does not produce expansion, and when expansion occurs in a carbonate aggregate, it is due to the ASR component of the rock, such as clay content or crypto-

---

* Corresponding author.
E-mail addresses: angel.lopez@aidico.es (A.M. López-Buendía), vcliment@grupogla.com (V. Climent).

0008-8846/$ - see front matter © 2006 Elsevier Ltd. All rights reserved.
doi:10.1016/j.cemconres.2006.05.032

crystalline quartz [6]. Nevertheless, Xu et al. [7] obtained expansion in carbonates (i.e., dolomite and limestone dolomite using (micro)concrete microbar), although the higher deterioration occurred in aggregates which contained clays. Using LiOH solutions in microbar tests, Qian et al. [8] determined expansion in carbonate aggregate, which was probably attributed to the ACR phenomena.

Although the production of carbonate aggregate is increasing, there is no efficient rapid testing procedure to predict AAR in carbonate rocks. Jensen et al. [9] have shown the need for the development of a petrographic method to solve these limitations.

AAR in carbonate aggregates has been related classically [1,10] to high clay content, dolomite/calcite ratio near 1 and small grain size. Most standards used are also related to argillaceous dolomitic dolostone in a fine matrix [11,12], making reference to the texture and impurities, as remarked Katayama [6]. On the other hand, the Spanish Standard UNE 146507 [13] is based on the geochemical composition of the aggregate, following the principle of stoichiometric balance of calcite and dolomite, which is made by means of the Ca/Mg ratio of the rock.

The stability of carbonate minerals in concrete is a function of the alkali content in high pH environment and their crystalline properties.

This paper is focused on the predictive evaluation of the hypothetical high risk of AAR in different carbonate rocks based on petrographic examination. The aim is to simplify and reduce time of testing with a preliminary selection of samples containing potentially reactive components.

Samples with high expected mineral instability have been collected, considering criteria of crystallinity and crystalline stability of carbonate minerals and silica content.

2. Background for sample selection

2.1. Silicification and its influence

Silicification in carbonate rocks can have several origins. Most of the silica in those rocks is biogenic by accumulation of siliceous organic remains, mainly radiolarites or diatomites, and sponge needles, with a subsequent diagenesis with chert formation and chert-replaced carbonates. Clay alteration, volcanic influence, silica rich waters or detritic silica, can be also produce it, see Ref. [14].

Silica content in carbonates, such as micro- and cryptocrystalline quartz, is considered very important for alkali-silica reaction (ASR) in carbonates; it is even classically considered as the principal [6]. The content of reactive silica in carbonates is very frequently difficult to determine. Berktas et al. [15], adding chert nodules to an inert carbonate, obtained reactivity from additions of 5–15%. Although texture was not considered, the results can be taken as an approach.

Silica content is equivalent to a pozzolanic reaction ($CaO–SiO_2–H_2O$), in which the size and specific surface influence in the reaction, changing the rate and the extent of the reaction and the scale [16,17]. Clay content in aggregates has been shown to react with alkaline [18,19].

2.2. Dedolomitization and its influence

The stability of carbonate minerals in the alkaline rich environment in concrete is a function of alkaline compounds [8]. The influence of the calc-alkaline compounds, such as portlandite, has been also studied as a dedolomitization agent in dolostone [20].

Dedolomitization is the classical process considered in carbonate aggregate [2]. During the reaction of dolomite, brucite is formed as a subproduct, having implications for the dimensional stability [6,21]. It is a very slow process in conditions with over-saturation in Ca of water, producing good stoichiometric calcite as resultant [22]. Calcite from dolomite transformation is also very selective, showing in those dolostone with lower stoichiometric dolomites (high relative Ca/Mg content) a more clear development [23]. This has been deduced in waters coming from sediments with calcite and dolomite, where Ca/Mg activity ratios are controlled by equilibrium between calcite and poorly ordered crystalline dolomite [24].

Calcite inclusions in dolomite crystals will depend on the diagenetic processes [25] and will have an influence over the dissolution and dedolomitization vulnerability [26]. Dolomite texture [27] will determine the phase stability in dolomites.

ACR evolution and kinetic rate are related with the aggregate texture of the carbonate rock which could produce expansion and have not been considered yet [28]. Nevertheless, Katayama [6] remarks that the results suggest that the degree of dedolomitization is a direct function of the dolomite crystal content and are not explained with texture influence. This conclusion is also supported using the example of the coarse-grained dolomite crystals of dolostone aggregates, which shows reaction rims and carbonate haloes.

Dolomite dissolution rate is very high during the first few days at room temperature with simulated solutions [29], but decreases with time.

In dolostone without silicate minerals, the expansion processes [30] are very unclear. The dimensional behaviour with concrete has been shown as following a complex pattern.

ACR expansion has been, however, related with the combination of two actions [6]: on one hand, the dedolomitization process, and on the other, the silicate compounds.

Clay content could contribute in the expansion coming from the interstitial brucite crystallization produced during dedolomitization [31].

3. Materials and methods

3.1. Carbonate aggregate samples

Selection of samples has been done following petrological criteria of stability of mineral assemblage and porosity. A selection of representative samples was done, as follows:

1. dolomite from dolomitization with relic calcite,
2. calcite from dedolomitization with relic dolomite,
3. iron and clays content in crystalline dolomite,

Table 1
Origin and lithology of carbonate rock samples

Sample	Lithology	Geological formation
CDD	Calcitic dolostone with dedolomitization	Cretaceous, Iberian Range
CD	Calcitic dolostone with partial dolomitization	Jurassic, Betic Range
FD	Ferric dolostone with clays with high porosity	Cretaceous, Iberian Range
CDX	Calcitic dolostone with chert	Cretaceous, Iberian Range
LX	Limestone with chert	Jurassic, Cantabrian Zone
C	Biosparite, limestone	Eocene, Betic Range

4. dolomite from dedolomitization with relic calcite and chert,
5. crystalline dolomite with high porosity and high iron content,
6. influence of the high porosity in dolostone.

A total of five lithologies of carbonate rocks has been selected to draw the basic pattern for the petrographic influence in the AAR study, including additionally a non-reactive limestone as control (Table 1).

Sample collection has been made using geological criteria and facies stratigraphical correlation in quarries and field outcrops. Aggregates were sampled in the specific strata after well-defined facies and lateral relationships.

Field sampling was done using a hammer, sledgehammer and digger machine depending on accessibility, around 150 kg of each sample was collected.

Samples were processed in a jaw crusher at 4–8 and 5–10 cm grain size.

3.2. Sample preparation for microscopy and SEM

A petrological study was made, giving the facies relationship in order to have an interpretative composition of the rock and to elucidate the potential stability of the mineral phases.

In addition, a representative amount of crushed samples were placed in solutions of 1 M LiOH and NaOH to study the mobilization and phase changes in the aggregates as a function of time. Samples of 4–8 mm diameter were stored at 80 °C, to simulate similar conditions to the accelerated mortar test explained below.

A treatment of alizarin red and fluorescent dye were systematically applied in half sample to have a family of samples with different treatments to study all the possibilities. The application of fluorescent dye epoxy resin and alizarin red in half sample was made following the methodology explained in Humphries [32]. Sample impregnation using acetone as previous treatment [33] was made, and vacuum condition of 150 mbar at 40 °C during 5 h, prior to injection of resin.

Table 2
Mortar bar dosages

Parameter	AAR-2	AAR-5	LiAAR-5
Water/cement ratio (by mass)	0.47	0.32	0.32
Aggregate/cement ratio (by mass)	2.25	1.0	1.0
Flow (mm)	205–210	150–155	150–155
Alkali equivalent (%)	–	1.5 Na eq.	1.5 Li eq.

Table 3
Water absorption

Sample	Water absorption
CDD	0.30%
CD	1.2–1.8
FD	3.36
CDX	1.42%
LX	0.5–1.0

Ordinary and polished thin sections were studied under a Zeiss Axioskop 40 polarising optical microscope with reflected and transmitted light and with a mercury lamp and blue filter. A Nikon stereo binocular microscope was used for evaluation of the aggregate.

For scanning electron microscope study, a Hitachi S-3000N with EDAX incorporated was used in working condition of 20 kV of accelerating voltage, vacuum environment of 10^{-5} Torr, beam current around 50–60 nA. EDAX showed a standard detection limit of 1 wt.% on polished surfaces and working in a focal length around 15 mm. Specimens were coated with graphite prior to examination.

3.3. Accelerated test methodology

The mechanical behaviour of mortar was evaluated using the dimensional stability in an ultra-accelerated mortar bar testing (UAMBT) in a hyper-saturated alkaline solution. As the influence of the type of alkaline solution [8] and other parameters [4,7] is significant, the selection of the procedures to evaluate dimensional stability has been multiple, as follows:

- UAMBT for detection of potential alkali-reactivity of aggregates, AAR-2 [34].
- rapid preliminary screening test for carbonate aggregate AAR-5 [35], based on Sommer [36] and Sommer et al. [37] using the recommendation of NaOH solutions.
- modification of AAR-5 using lithium hydroxide (LiAAR-5) instead of sodium hydroxide.

According to note 2 from the RILEM AAR-5 method, reference cement from Norcem was employed in this research (alkali content of 1.25 wt.% of Na equivalent; density of 3.12 kg/m^3). Mixing procedure followed UNE-EN 196-1 [38]. Dosages used are shown in Table 2.

Table 4
Particle size distribution of aggregates

Grain size (mm)	8/6.3	6.3/5	5/4	4/2	2/1	1/0.5	0.5/0.25	0.25/0.125
AAR-2 (%)				10	25	25	25	15
AAR-5; LiAAR-5 (%)	33	33	34					

Water absorption of the aggregates was measured following UNE-EN 1097-6 [39]. The result of two samples are summarised in Table 3.

The grain size distribution of the crushed aggregates for the tested methods are exposed in Table 4. Grain size range was delimited by the AAR2 (0.125–4 mm) and AAR-5 (4–8 mm).

The moulds with the test specimens were placed in the storage room (20 °C; 100% of relative humidity) for a period of 24 ± 2 h. After demoulding, a first measurement was taken (l_1). The mortar bars were stored in a container with distilled water at 80 ± 2 °C for a period of 24 h. A second measurement was then taken (l_0). After that, the bars were immersed in solution 1 M NaOH or LiOH, preheated at 80 ± 2 °C and stored during 28 days.

4. Results

4.1. Aggregate petrography

4.1.1. Calcitic dolostone with dedolomitization (CDD)

The rock is mostly constituted by a facies of calcite dolostone with signs of dedolomitization (Fig. 1). A facies of limestone of dedolomitization is also associated. The proportion of the dolomitic limestone of dedolomitization is around 30% of the total.

The facies of calcite dolostone shows a range of dedolomitization from dolomite partially dedolomitized up to dolomitic limestone. Euhedral dolomite crystals show a marked zonation, usually with a core dense in inclusions with a composition rich in iron. In facies richer in calcite from dedolomitization, the euhedral morphology or the relict rhomb of the dolomite precursor is conserved, having zoned dedolomite. The texture shows a selective dedolomitization by bands. The inclusions are eventually conserved, having calcite with a structure of very well- conserved pseudomorphs of dolomite.

The porosity of the rock is from moderate to high, with fabric selective of intercrystal type, and non-fabric-selective vuggy porosity. The intercrystal/vug porosity ratio is in direct proportion of dolomite/dedolomite ratio. Some veins of secondary calcite fill porosity associated with fractures.

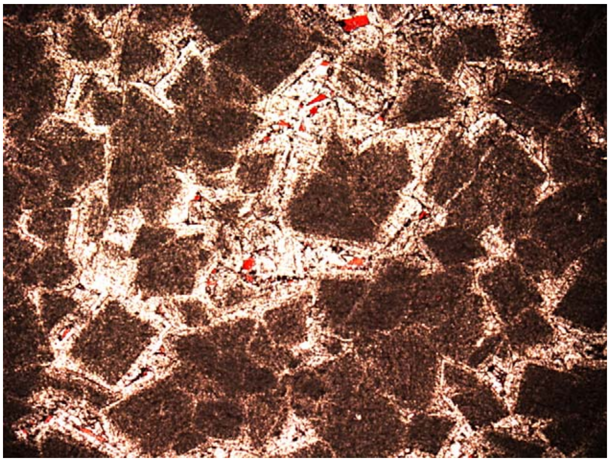

Fig. 1. Dolomite affected by an incipient dedolomitization. Core shows a cloudy texture rich in inclusion with micritic dolomite and a composition rich in iron. Cross-polarised light, horizontal field of view 5 mm.

Fig. 2. Sucrose dolostone with coarse subhedral (planar-s) dolomite with slight zonation. Iron oxides are relatively abundant in all the samples, which tend to be located in bands. Cross-polarised light, horizontal field of view 1.25 mm.

The bulk of the rock has 90% of dolomite and 10% of dedolomite calcite.

4.1.2. Calcite dolostone (CD)

The rock is made up of a composition of calcitic dolostone with minor content in clays (<5%). Three types can be distinguished: (1) brecciated dolostone, (2) dolomitic limestone and (3) calcitic dolostone.

Calcite dolostone is the most abundant type. It is a non-depositional texture with well-crystallized euhedral rhombohedral dolomite (planar-e). Some remains of calcite can be found, although most of the calcite found is of secondary origin.

4.1.3. High-porosity ferric dolostone with clays (FD)

The rock is a dolostone with a high content in iron oxides and some quartz. Dolomite has a sucrose texture with crystals showing subhedral of planar type (planar-s) fabric. Zoning in dolomites with a core containing inclusions is present. Iron oxides are filling some crystal contact in the bulk of the rock, although it can be distributed in bands or zones with higher content (Fig. 2). In reflected light over a polished block and with mercury lamp, it is possible to differentiate between amorphous iron oxide (yellow colour) and hematite (red-violet to wine red).[1] Clay content appears as a minor component with a proportion slightly under 5 vol.%. Secondary calcite is filling some fractures.

The rock shows a high vuggy porosity with minor intercrystalline porosity.

---

[1] Colour is clearly a critical element of the techniques used in this study, so the text and images of this paper have not been modified to reflect the fact that images in *Cement and Concrete Research* are printed in black and white. A full colour copy of this paper is available online at www.sciencedirect.com/.

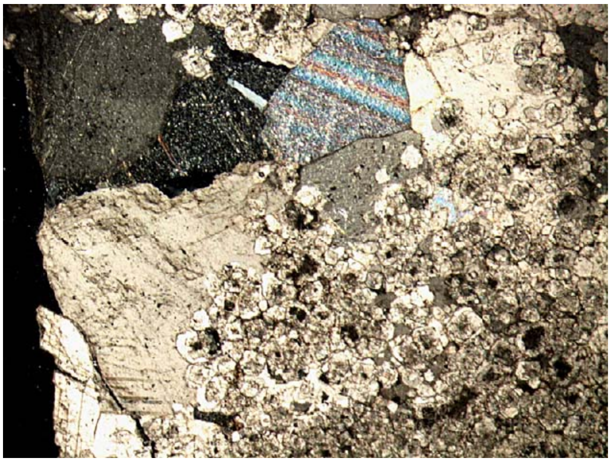

Fig. 3. Calcite recrystallisation by dedolomitisation showing zonation with a very well preserved planar-s fabric, with a sucroid texture. Secondary calcite is also filling vugs. Cross-polarised light, horizontal field of view 5 mm.

4.1.4. Calcite dolostone with chert (CDX)

Lithologically, the rock varies in composition from dolostone with chert to calcite dolostone with chert nodules and some dispersed micro- and crypto-crystalline silica.

Sampling was made over massive part forming the top of the dolomitic lithological unit. The dolomitization degree increases toward the bottom and appear chert and silicified dolostone in the middle part of the set.

The obtained aggregate is made up of calcitic dolostone and limestone of dedolomitization and calcite dolostone. The texture of dolomite is mostly euhedral with the grain contact of planar-e type and also appears subhedral dolomite and dedolomite with crystal face of planar-e type (Fig. 3) in the stratigraphically upper part. Calcite/dolomite proportion is around 0.6, considering primary calcite, dedolomite calcite and secondary calcite.

Chert is made up of crypto- and micro-quartz, having a significant amount of iron oxides. The porosity of the nodules is visible by microscope. Also, there is silicification in the whole mass of the calcitic dolostone.

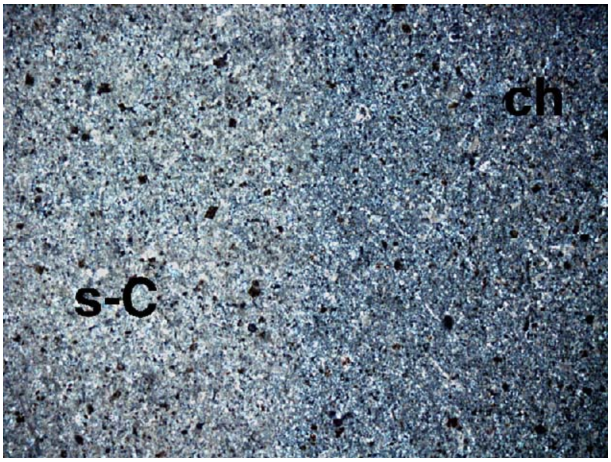

Fig. 4. The micrograph shows a limestone intensely silicified on the left part (s-C), and a micro- and cryptocrystalline quartz with calcite remains on the right (ch). Boundaries between the tow parts are not clear with diffused band. Cross-polarised light, horizontal field of view 5 mm.

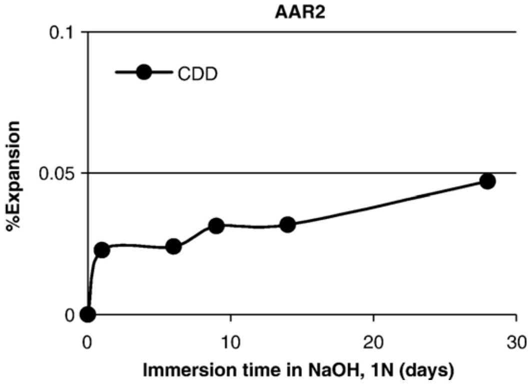

Fig. 5. Mortar bar expansion following AAR2. Aggregate CDD.

The amount of silica of the aggregate is around 8 vol.%.

4.1.5. Limestone with chert (LX)

The rock is a limestone with chert, made up of calcite of recrystallisation and iron-rich dedolomite with a layer rich in chert nodules.

Limestone can be classified as a partially silicified biosparite, with a neomorphic fabric of aggrading calcite cement crystals which has microsparite and pseudosparite. Secondary micro- and crypto-crystalline silica is affecting part of the microsparite cement. This replacement also appears in fossils moulds (Fig. 4). Isolated pseudomorphic calcite with euhedral to subhedral morphology is partially corroded.

Centimetre- to decimetre-sized chert nodules consist of fine-grained crystalline quartz (4–60 μm), possibly also containing some crypto-crystalline silica <4 μm.

4.2. Ultra-accelerated mortar bar testing (UAMBT)

Results of the accelerated mortar and micro-concrete bars show very significant differences depending on the method used (Figs. 5–10).

In general, the differences in dimension change are more evident in the AAR-5 test, in agreement with Sommer et al.

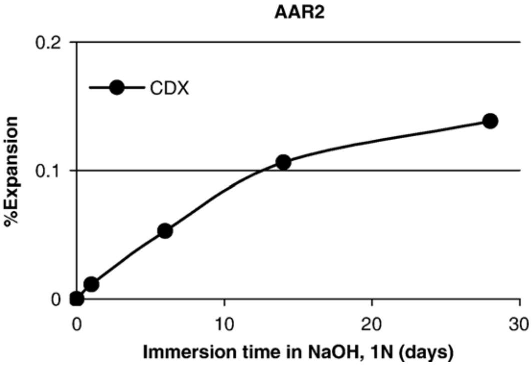

Fig. 6. Mortar bar expansion following AAR2. Aggregate CDX.

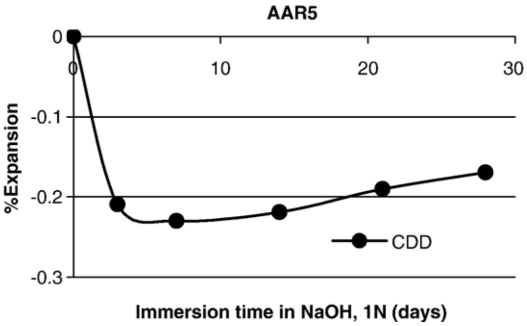

Fig. 7. Microconcrete prisms expansion following AAR5. Aggregate CDD.

[40]. The AAR-2 test shows expansion when unstable silica minerals in alkali environment are present, showing good efficiency when ASR is involved. In contrast, in the absence of silica components, the expansion of AAR-2 is very low.

Results of the AAR-5 test shows a significant relative dimension change in the presence of dolomite, except in the case of CD aggregate. Aggregate CDD shows an increasing expansion throughout the test time, although only 0.05% was obtained after 28 days of testing. FD aggregate exhibits similar behaviour showing minor expansion. Aggregates with chert show continuous expansion with 0.14% in CDX and a spectacular 0.4% in LX.

In the AAR-5 test, the trend is apparently contradictory in some samples. In CDD aggregate, a strong shrinkage takes place, with a maximum of −0.23%, having a subsequent relative expansion, with an overall net shrinkage after 28 days of −0.17%.

In CDX aggregate, the shrinkage is evident within the first 3 days, −0.15%, showing a subsequent strong expansion with a final expansion of 0.12% after 28 days. The shrinkage could be considered as an unstable mechanical behaviour.

CD aggregate, on the contrary, shows very low expansion at 28 days (0.015%).

Using the variation LiAAR-5 (similar to AAR-5, using 1 M LiOH solution), the results are very low in the tested CDD and CDX samples. Both aggregates exhibit very similar petrographical dolomite textures, with the difference of the silica chert content in CDX.

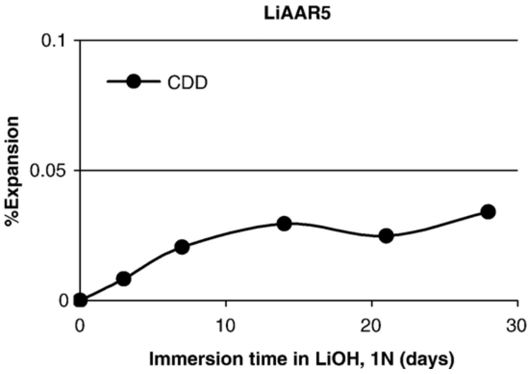

Fig. 9. Microconcrete prisms expansion following LiAAR5. Aggregate CDD.

4.3. Immersion in alkaline solution

Aggregates in alkaline solutions of LiOH and NaOH at a concentration 1 M show interesting results.

In samples without silica, the transformation is not very significant and it is very difficult to demonstrate. The main aspect is mobilization of iron which suffers a migration in the borders giving small rims, which can be observed in alkaline environment of concrete [41].

In general, after the alkali leaching the rock suffers a general diffusion, making the aspect of dirty thin section. Nevertheless, euhedral or subhedral dolomite rhombs of dedolomite pseudomorphs, as well as calcite, show no measurable changes. This is the situation of CDD (Fig. 11), CD (Fig. 12) and FD samples.

Aggregates with chert show a clear alteration, affecting not only the silica but also the micro-carbonate and iron. Using NaOH solutions, silica in aggregates are affected, having a partial dissolution with a gelification process, which is partially removed from the sample. The iron is also mobilized and appears as a diffused dark mask (Figs. 13 and 14). This phenomenon can be observed at 3 days and is very evident at 7 days. At 28 days, the alteration rims affect to 2 mm depth from surface.

Using 1 M LiOH solution, the change exhibits clear differences. The removed micro- and crypto-crystalline quartz is very low and the external rimed zone appears clean under the microscope. A small rim of iron oxides affect the border, without

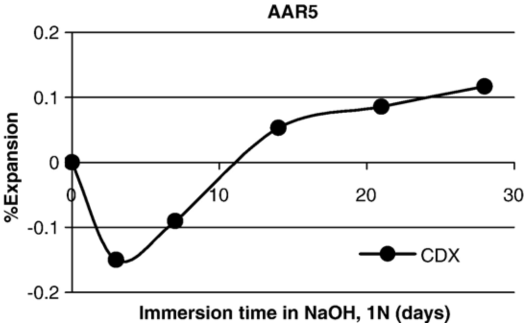

Fig. 8. Microconcrete prisms expansion following AAR5. Aggregate CDX.

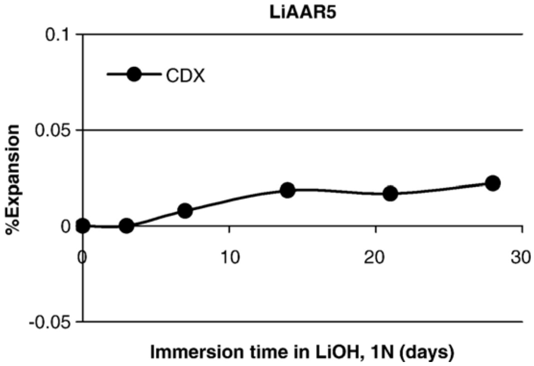

Fig. 10. Microconcrete prisms expansion following LiAAR5. Aggregate CDX.

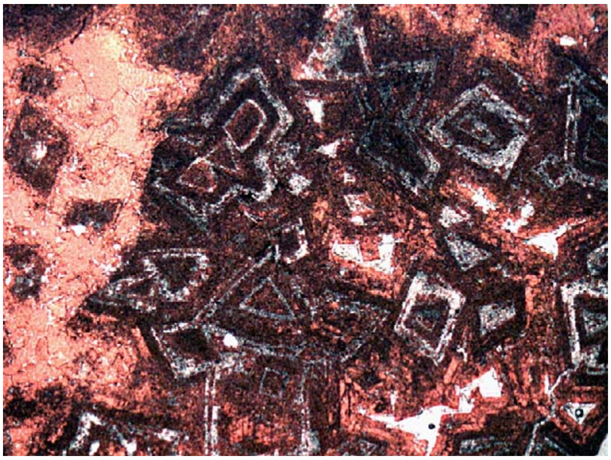

Fig. 11. CDD aggregate after 7 days in NaOH. Sample stained with Alizarin-red. There are no significant alterations in dolomite using this technique. Cross-polarised light, horizontal field of view 5 mm.

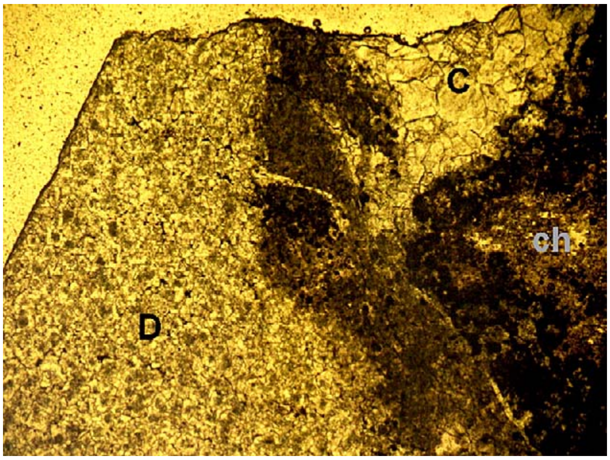

Fig. 13. CDX aggregate after 28 days in NaOH. An alteration band is evidenced in dolomite facies (D) in contact with the chert (ch). Chert also shows double rim of iron oxides. Plane-polarised light using blue filter, horizontal field of view 5 mm.

migration toward the inner part of the aggregate grain (Figs. 15 and 16).

Brucite formation in this sample has been evidenced (Fig. 17).

5. Discussion

As the dimensional instability in the concrete due to AAR is produced by the reaction between the alkali cement and the component of the aggregate, the study has been based on the stability of the mineral phases content in the rock.

Carbonate mineral stability can be used as criteria for AAR diagnosis by a petrographical test of carbonate aggregates, as has been summarised in Table 5.

5.1. Dolomite from dolomitization with relic calcite

Dolomite from dolomitization has shown some alteration. This transformation, however, has been observed indirectly with the presence of brucite by SEM (Fig. 17) and with a Mg-rich hydrated calcium silica and alumina amorphous component in the mortar. Using only the expansion test, the instability has not been properly demonstrated. This conclusion is in agreement with the results of [6].

5.2. Partial dedolomitization with relic dolomite

Dolomite partially dedolomitized, exhibits a very evident transformation after alkali solution treatment with a subsequent mechanical implication on the structure. In the sample with dolomite and calcite of dedolomitization only (CDD), the mechanical implication for the concrete is mainly due to shrinkage.

The explanation of the shrinkage could be attributed to the more compacted structure conferred by Mg instead of Ca, having Mg–O lower interatomic distance than Ca–O.

The level of calcite/dolomite proportion needed to have mechanical implications in the concrete has not been shown accurately. An incipient induced dedolomitization on the dolomitic fabric, however, demonstrates a clear instability of the crystalline phases.

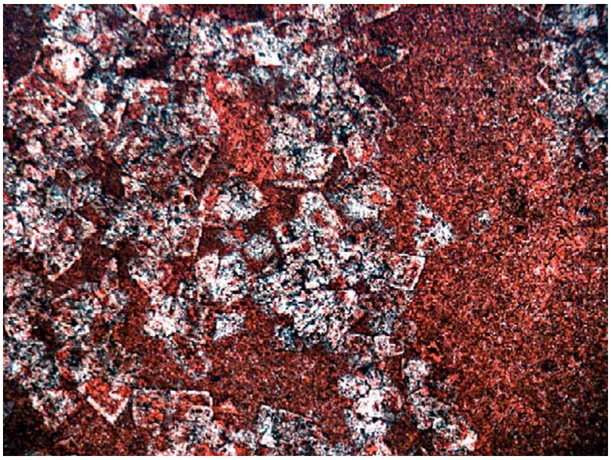

Fig. 12. CD aggregate after 7 days in NaOH. There are no consistent alterations, although an apparent diffusion appear in the crystal border. Sample stained with Alizarin-red. Cross-polarised light, horizontal field of view 1.25 mm.

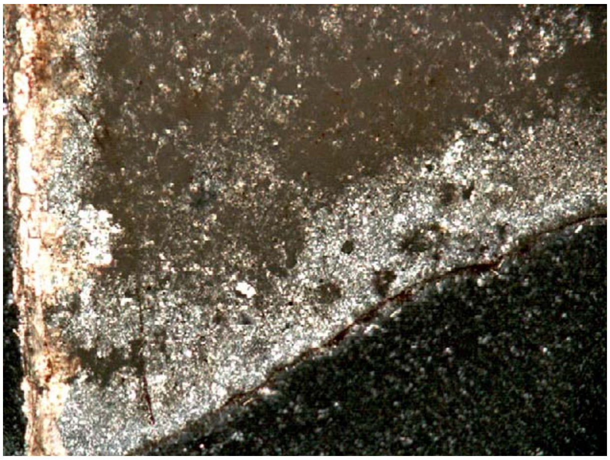

Fig. 14. LX aggregate after 28 days in NaOH 1 M. There is a strong mobilization of iron forming rings, and partial solution of crypto-quartz. Cross-polarised light, horizontal field of view 5 mm.

Fig. 15. CDX aggregate after 28 days in LiOH 1 M solution. Iron oxide is concentrated in the centre of the chert and just at the border. Cross-polarised light, horizontal field of view 5 mm.

5.3. Iron and clays content in crystalline dolomite

Iron oxides not necessarily react easily with cement. Nevertheless, they could be used indirectly as a resultant component of an alteration of the rock. The mobilization of iron oxides in aggregates in alkaline solution also demonstrates this phenomena. Iron oxides in the samples appear with intercrystalline distribution and in inclusions. Partially, they are liberated by dissolution or transformation of minerals, and partially mobilized as alkaline complexes.

In that sense, iron oxide content can be used, with petrological caution, as criteria of instability of mineral phases when other potential components appear. In NaOH or LiOH test for aggregate, the mobilization of iron appears as a criteria of potential reactivity diagnosis.

Clays can react with alkalis, mainly smectite, but also in other clay minerals [19]. With temperature or diagenesis, the instability of silica segregation increases in proportion with the reactivity of the sub-products of this transformation.

5.4. Chert content in the carbonate rock

Chert is an important ASR component. It could be for guidance of the value of chert content of 5–15% to be considered as reactive [15].

The rim thickness in aggregate after alkaline test can affect up to 2 mm thickness at 28 forming gels [42], evidence of its reactivity with cement.

5.5. Partially dedolomitized dolomite with calcite remains and chert

In the presence of dolomite with dedolomite and chert, the expansion test has demonstrated an overlapping of both phenomena (Fig. 8). The fast shrinkage proportioned by induced dedolomitization effect is overlapped, without any apparent interaction, with the lower expansion of the ASR of the chert. This type of aggregate runs a particularly high risk of AAR.

Fig. 16. LX aggregate after 28 days in LiOH 1 M. There is a significant alteration with partial carbonate alteration. It shows an alteration rim of 1.5 mm with external iron oxide rims near the borer. Cross-polarised light, horizontal field of view 5 mm.

5.6. Influence of the porosity, crystalline dolomite with high porosity and high iron content

Well-crystallized dolomite without any signs of dedolomitization has good stoichiometry and is consequently stable in alkaline media during the test period.

Although porosity can accelerate the reaction by having a higher specific surface and more ionic mobilization capability, this is not enough to have reactivity. Nevertheless, any potentially reactive component in the aggregate has better access and better ionic exchange in porous rocks, and as a consequence, a low proportion of this potential reactive component is very significant. For example, FD aggregate has theoretically less than 5% of potential components (clays) and has significant expansion results. It can be explained by the very high porosity.

By taking the results from the studied rock as aggregates, a table has been elaborated (Table 6) summarising the parameters considered to be used as a petrographic approach for predictive diagnosis of AAR.

With criteria of Table 5, and using the diagnosis components of Table 6, a lithological classification of aggregates has been

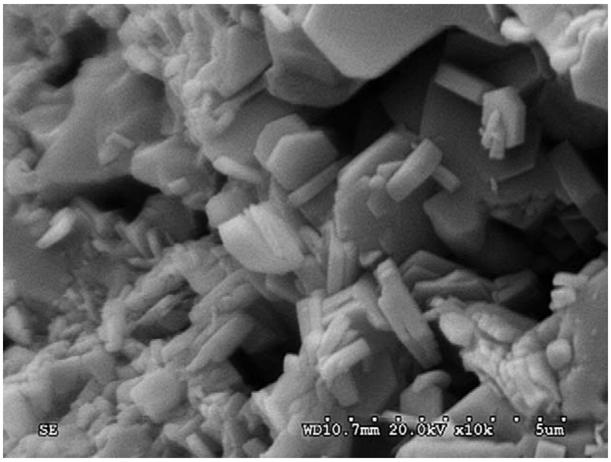

Fig. 17. Brucite accumulation in CDX sample after UMBT (AAR-2) treatment.

Table 5
Summary of tests applied on the selected aggregates

Aggregate	Aggregate type	Chemical test[a]	Expansion test	AAR-1	Carbonate mineral stability	Porosity	Type of reaction
CDD	Calcite dolostone with dedolomitization	Potentially reactive	Shrinking	Class I	Very unstable	Very low	Induced dedolomitizaton
CD	Calcite dolostone with dolomitization	Potentially reactive	Stable	Class I	Unstable	Moderate to high	None
FD	High-porosity ferric dolostone with clays	Non-reactive	Expansive	Class I	Stable; iron oxide unstable	Very high	Weak induced dedolomitization-ASR
CDX	Calcite dolostone with chert	Potentially reactive	Expansive	Class II	Unstable	Moderate	ASR and induced edolomitization
LX	Marly limestone with chert	Non-reactive	Expansive	Class II	Stable	Low to moderate	ASR

[a] UNE 146507-2, showing the Ca/Mg in rock bulk stoichiometry deviation from calcite or dolomite.

elaborated, which is summarised in Table 7, and following the philosophy and trend of the RILEM AAR-1 [9].

6. Conclusions

A selection of samples using criteria of mineral phases instability contained in the rock was carried out. An accelerated test for aggregate instability with alkaline solution, together with the accelerated mortar and micro-concrete bar tests, has allowed a petrographic classification of aggregates to be drawn up according to the AAR risk.

Induced dedolomitization shows very significant shrinkage behaviour in laboratory tests, macroscopic scale implication in concrete is, however, not very well known.

Table 6
Diagnosis of components, fabric and texture with signs of high risk of AAR in carbonate aggregate

Parameter	Description	Example	AAR
Porosity	Vug	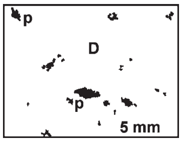	Basic criteria, increase the efficiency of any other component
(Partial) Dedolomitization	Mainly when is selective and zoned	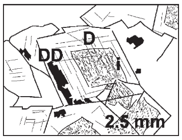	Produce shrinkage by induced dedolomitization with cement
Partial dolomitization	Mainly when produce zoned dolomite with high inclusions content		Produce shrinkage by induced dedolomitization with cement
Microcrystalline and cryptocrystalline quartz in nodules	Nodules with porous aspect in fluorescent stain	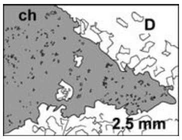	Produce expansion
Disperse microcrystalline and cryptocrystalline quartz	In bands, micro-nodules or filling organic moulds. Opaline fossils.	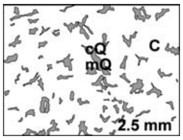	Produce high expansion
Iron oxide content	In bands, concentrated in zones filling porous.	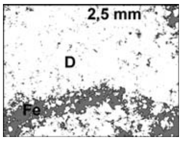	Associated indirectly to expansion phenomena
Clays			Associated to expansion

Examples are drawn directly from samples at scale.
DD, dedolomite (calcite from dedolomitization); D, dolomite; p, porosity; C, calcite; ch, chert; cQ-mQ, crypto and micro-crystalline quartz; Fe, iron oxides.

Table 7
Classification in groups of alkali-carbonate aggregate reactive risk, according to results and by extension of the obtained results

Classification	Reactivity	Lithology
I	Non-reactive	Limestone Dolostone with calcitic cement Dolostone
II	Potentially reactive	Calcitic dolostone with partial dedolomitization Dolomitic limestone with partial dolomitization Limestone and marly limestone with chert
III	Reactive (probable reactivity)	Type II + clay-rich content Type II + micro- and crypto-crystalline quartz Type II + microcrystalline dolostone Silicified marly limestone

Data demonstrate that ACR in non-silica content carbonates is produced by the instability of the carbonate minerals, causing induced dedolomitization in the concrete environment rich in alkali, which depends on the grain size and stoichiometry of dolomite.

AAR in carbonate aggregate can have a combination of induced dedolomitization and ASR in agreement with Katayama [5,6].

A simple rule for a petrographic approach to predict AAR in carbonate aggregate can be suggested (Table 7) using criteria of mineral stability based on crystal size, crystal shape, dedolomitization, dolomitization and zoned dolomite.

The criteria of non-silica ACR risk can be summarised as follows:

- incipient or developed dedolomitization;
- very zoned dolomite;
- medium developed dolomitization with zoned dolomite;
- additional textural criteria (such as high porosity or iron oxide rims content).

Criteria of ASR risk in carbonate aggregate can be summarised as follows:

- partial dispersed silicification;
- presence of chert nodules presence with micro- and crypto-crystalline quartz;
- altered clays content.

The aim of the classification table obtained is to simplify the evaluation of the AAR risk in carbonate aggregate by using a preliminary petrographical test. The proposed classification has been oriented following the terminology of RILEM AAR1 in I non-reactive, II potentially reactive and III reactive (probable reactivity).

Acknowledgments

This paper has been mainly financed by the ARICAR Project (INMRMA/2004/8) for the ARIVAL association with the support of the Spanish regional government of Generalitat Valenciana, and with contribution from the PARTNER project (GRD1-2001-40103 PARTNER) team. We are grateful for the help in the needs and suggestions to the RILEM Committee TC191ARP and the Carbonate Group for Task group on Petrography of Carbonate Rocks. We are also grateful to Dr. H. Sommer and Dr. T. Katayama for their critical comments and suggestions contributing to the improvement of the paper.

References

[1] E.D. Swenson, J.E. Gillott, Characteristics of Kingston carbonate rock reaction, Highw. Res. Board, Bull. 275 (1960) 18–31.

[2] D.W. Hadley, Alkali reactivity of carbonate rocks—expansion and dedolomitization, Highw. Res. Board, Proc. 40 (1961) 462–474.

[3] J.E. Gillott, Mechanism and kinetics of expansion in the alkali-carbonate rock reaction, Can. J. Earth Sci. 1 (1964) 121–145.

[4] L. Tong, M. Tang, Expansion mechanism of alkali-dolomite and alkali-magnesite reaction, Cem. Concr. Res. 21 (1999) 361–373.

[5] T. Katayama, A critical review of carbonate rock reaction—is there reactivity useful or harmful, in: A.B. Poole (Ed.), Proc. 9th International Conference on Alkali-Aggregate Reaction in Concrete, Concrete Society, London, UK, 1992, pp. 508–518.

[6] T. Katayama, How to identify carbonate rock reactions in concrete, Mater. Charact. 53 (2004) 85–104.

[7] Z. Xu, X. Lan, M. Deng, M. Tang, A new accelerated method for determining the potential alkali-carbonate reactivity, Cem. Concr. Res. 32 (2002) 851–857.

[8] G. Qian, M. Deng, M. Tang, Expansion of siliceous and dolomitic aggregates in lithium hydroxide solution, Cem. Concr. Res. 32 (5) (2002) 763–768.

[9] V. Jensen, T. Katayama, B. Fournier, Rilem AAR-1 petrographic method: Carbonate Working Group, in: J.J. Hughes, A.B. Leslie, J.A. Walsh (Eds.), Proc. 10th Euroseminar on Microscopy Applied to Building Materials, University of Paisley, Scotland, UK, 2005.

[10] M.A. Ozol, Alkali-carbonate rock reaction. Significance of tests and properties of concrete and concrete-making materials, ASTM STP 169C, in: P. Klieger, J.F. Lamond (Eds.), American Society for Testing and Materials, Philadelphia, 1994, pp. 372–387.

[11] CSA A23.1-94, Concrete Materials and Methods of Concrete Construction, Appendix B Alkali-Aggregate Reaction, Canadian Standars Association, Mississauga, ON, Canada, 1994.

[12] ASTM C294-98, Standard descriptive nomenclature for constituents of concrete aggregates, Annual Book of ASTM Standards, vol. 0402, American Society for Testing and Materials, West Conshohocken, PA, 1998.

[13] UNE 146507-2EX, Test for aggregates. Determination of the potential reactivity of aggregates, Chemical Method. Part 2: Determination of the Alkali-Carbonate Reactivity. Norma Española, Asociación Española de Normalización y Certificación AENOR, 1999.

[14] R. Hesse, Silica diagenesis: origin of inorganic and replacement cherts, Earth-Sci. Rev. 26 (1989) 253–284.

[15] F. Berktas, L. Turanli, T. Topal, M.C. Goncuoglu, Alkali reactivity of mortars containing chert and incorporating moderate-calcium fly ash, Cem. Concr. Res. 34 (2004) 2209–2214.

[16] X. How, L.J. Struble, R.J. Kirkpatrick, Formation of ASR gel and the roles of C–S–H and portlandite, Cem. Concr. Res. 34 (2004) 1683–1696.

[17] V. Climent, A.M. López-Buendía, P. Verdú, P. Martí. (2004). Development of a methodology to prevent alkali-carbonate reaction for aggregate exploitation management. Arival-Generalitat Valenciana, unpub. Report, 2004.

[18] M. Choquette, M.A. Bérubé, J. Locat, Mineralogical and microtextural changes associated with lime stabilization of marine clays form eastern Canada, Appl. Clay Sci. 2 (1987) 215–232.

[19] C. He, E. Makovicky, B. Osbaek, Thermal stability and pozzolanic activity of raw and calcined mixed-layer mica/smectite, Appl. Clay Sci. 17 (2000) 141–161.

[20] S. Galí, C. Ayora, P. Alfonso, E. Tauler, M. Labrador, Kinetics of dolomite–portlandite reaction: application to portland cement concrete, Cem. Concr. Res. 31 (2001) 933–939.

[21] E. García, P. Alfonso, M. Labrador, S. Galí, Dedolomitization in different alkaline media: application to Portland cement paste, Cem. Concr. Res. 39 (9) (2003) 1443–1448.

[22] C. Ayora, C. Taberner, M.W. Saaltink, J. Carrera, The genesis of dedolomites: a discussion based on reactive transport modeling, J. Hydrol. 209 (1–4) (1998) 346–365.

[23] A. Katz, Calcian dolomites and dedolomitization, Nature 217 (1968) 439–440.

[24] K. Hyeong, R.M. Capuano, Ca/Mg of brines in Miocene/Oligocene clastic sediments of the Texas Gulf Coast: buffering by calcite/disordered dolomite equilibria, Geochim. Cosmochim. Acta 65 (2001) 3065–3080.

[25] D.F. Sibley, Climatic control of dolimitization, Seroe Domi Formation (Pliocene), Bonaire, in: D.H. Zenger, J.B. Dunham, L. Ethington (Eds.), Concepts and Models of Dolomitization, Soc. Econ. Paleontologist Mineralogist, vol. 28, 1980, pp. 247–258.

[26] F. Thériault, I. Hutcheon, Dolomitization and calcitization of the Devonian Crosmont Formation, northern Alberta, J. Sediment. Petrol. 57 (1987) 955–966.

[27] D.F. Sibley, J.M. Gregg, Classification of dolomite rock texture, J. Sediment. Petrol. 57 (1987) 967–975.

[28] G. Qian, M. Deng, X. Lan, Z. Xu, M. Tang, Alkali carbonate reaction expansion of dolomitic limestone aggregates with porphyrotopic texture, Eng. Geol. 63 (2002) 17–29.

[29] E. García, C. Ayora, P. Alfonso, E. Tauler, S. Galí, Surface alteration of dolomite in dedolomitization reaction in alkaline media, Cem. Concr. Res. 39 (2003) 1449–1456.

[30] D. Min, T. Mingshu, Mechanism of dedolomitization and expansion of dolomitic rocks, Cem. Concr. Res. 23 (1993) 1397–1408.

[31] N. Tang, Z. Liu, S. Han, Mechanism of alkali-carbonate reaction. Concrete alkali-aggregate reactions, in: P.E. Grattan-Bellew (Ed.), Proc. 7th International Conference of Alkali-Aggregate Reaction in Concrete, Noyes Publ., Park Ridge, New Jersey, 1987, pp. 275–279.

[32] D.W. Humphries, The preparation of thin sections of rocks, minerals and ceramic, Royal Microscopical Society, Oxford Sci. Publ. Microscopy Handbooks, vol. 24, 1992.

[33] A.M. López-Buendía, A new method for the preparation of peat samples for petrographic study by transmitted and reflected light microscopy, J. Sediment. Petrol. 68 (1998) 214–217.

[34] RILEM, RILEM TC 106-AAR (AAR-2) "Detection of potential alkali-reactivity of aggregates—The ultra accelerated mortar bar test" Draft method 2002.

[35] RILEM (2004): RILEM TC ARP AAR-5, Rapid Preliminary Screening Test for Carbonate Aggregates, version April 2004, RILEM TC 191-ARP, Draft method 2004.

[36] H. Sommer. (2000): Ultra-accelerated Tests for Alkali-aggregate Reactivity: the RILEM and the Chinese Microbar Test Compared on Some Aggregates, report to RILEM TC 191-ARP (unpublished), Vienna 2000.

[37] H. Sommer, J. Steigenberger, U. Zückert, Vermeiden von Schäden durch Alkalizuschlagreaktion. Schriftenreihe Straßenforschung Heft 504, Bundesministerium für Verkehr, Innovation und Technologie 2001.

[38] UNE EN 196-1, Methods of testing cement. Part 1: Determination of strenght, AEN/CTN 80, AENOR, 1996.

[39] UNE EN 1097-6, Tests for mechanical and physical properties of aggregates. Part 6: Determination of particle density and water absorption, AEN/CTN 146, AENOR 2003.

[40] H. Sommer, P. Grattan-Bellew, T. Katayama, M.S. Tang, Development and inter-laboratory trial of the rilem AAR-5 rapid preliminary screening test for carbonate aggregates, 12th International Conferences of Alkali-Aggregate Reaction in Concrete, 2004.

[41] K.K. Aigizaki, M.J. De Rooij, D.D. Macdonald, Analysis of iron oxides accumulating at the interface between aggregate grains and cement paste, Cem. Concr. Res. 30 (2000) 1941–1945.

[42] D. Bulteel, E. García-Díaz, C. Vernet, H. Zanni, Alkali-silica reaction. A method to quantify the reaction degree, Cem. Concr. Res. 32 (2002) 1199–1206.